The effects of confinement and surface interactions on coexistence in a binary polymer mixture

Andrzej Budkowski,[a] Ullrich Steiner, and Jacob Klein
Department of Materials and Interfaces, The Weizmann Institute of Science, Rehovot 76100, Israel

(Received 16 March 1992; accepted 8 June 1992)

We have measured the composition-distance profile across a film consisting of two thin layers (200–600 nm) of a model binary isotopic mixture of deuterated polystyrene (dPS) and protonated polystyrene (hPS), coexisting with each other near their equilibrium compositions below the critical temperature for phase demixing for this pair. Profiles were determined normal to the silicon wafer on which the bilayer is mounted using nuclear reaction analysis, both for an uncoated silicon surface and for one coated with a gold layer. Measurements reveal that when both layers are thick relative to the characteristic width w (~ 100 nm) of the interfacial region between them, the coexisting compositions about the interface are close to their bulk values as determined earlier for this system. When the dimensions of the layers are made comparable with w, however, interactions with the confining surfaces may significantly modify the composition profile of the coexisting layers about the interface. This effect is marked at the polymer/silicon interface as a result of its interactions with one of the components (dPS), but is absent for a gold-coated surface in an identical geometry due to the much weaker influence of the surface. Our results are discussed in detail in terms of mean-field models of mixing in polymeric mixtures, and enable quantitative determination (using a Cahn construction approach) of the interaction parameters both at the polymer–air and polymer–silicon interfaces. Though we are not able to calculate in a completely *a priori* fashion the coexistence profiles as a function of the film thickness, we propose an approximate approach which provides good agreement of calculated composition profiles with those determined experimentally over the range of parameters in our experiments.

I. INTRODUCTION

The dynamic and thermodynamic properties of liquids, and in particular liquid mixtures, may be strongly modified by the effects of their confinement to narrow pores or films.[1–6] Qualitatively, this may be expected to occur for a number of reasons. (a) Ordering may be induced near the interface (such as a solid–liquid or solid–solid interface) by local surface fields or epitaxial effects; this is also related to the inducement of glassy behavior in the near-interface regions.[7] (b) For molecules near an interface, a lower "coordination number" of a given species with its own kind may change the overall free energy of the sample.[8] (c) Both short- and long-ranged surface fields may influence the energies of surface-adjacent molecules.[9] (d) For a binary mixture, one of the species may adsorb preferentially at the interface. To be specific, we discuss the case of thin films consisting of binary mixtures on a planar solid surface. The effects discussed above can then differ at the air–film (or vacuum–film) and at the film–substrate interfaces. More generally, one expects the effects of confinement to become important whenever the film dimensions become comparable with, or smaller than the relevant decay lengths of the surface fields or—for the case of preferential adsorption from a mixture—of compositional variations near the surface.

Theoretically, the question of the phase behavior of binary fluid mixtures in thin films has been studied by a number of workers.[3–6] Fisher and de Gennes[4] discussed the effect of the coupling between the increase in correlation lengths of composition fluctuations in a binary mixture near its critical point, the surface enrichment due to preferential adsorption of one of the components, and the overall composition in a thin liquid film of the mixture. Fisher and Nakanishi[5] considered the effect on the thermodynamic behavior in thin films of both purely geometric finite-size effects [e.g., (b) and (c) above] and effects arising from preference of the surface to one of the components in a binary system confined between two walls.

Experimentally, the effect of confinement to thin films on the thermodynamic behavior of binary mixtures has been studied through investigations of the shift in critical temperature T_c for phase separation in thin films relative to its value in the bulk. Mockler and co-workers have studied this shift in a binary small-molecule liquid mixture,[10,11] while Cohen and Reich[12,13] studied the variation of the phase-separation temperature in a thin film (confined between two plates) composed of a mixture of two polymers. In these studies, shifts were observed in T_c (or in the onset of cloudiness) as a function of both film thickness and of different confining surfaces.

In the present paper, we describe a study of coexisting polymer phases confined to a thin film on a planar solid substrate. In particular, we investigate the effect of the film thickness and the nature of the substrate on the composition of the coexisting phases normal to the solid surface.

[a]On leave of absence from the Jagellonian University of Krakow, Poland.

 0021-9606/92/195229-10$006.00 © 1992 American Institute of Physics

Downloaded 24 Jun 2007 to 132.77.4.129. Redistribution subject to AIP license or copyright, see http://jcp.aip.org/jcp/copyright.jsp

The use of flexible polymers to study binary mixtures presents a number of advantages from an experimental point of view. The dynamics of polymer chains are extremely sluggish due to their size and to entanglement effects, enabling the variation with time of the properties of thin films to be followed conveniently.[14] Second, in the context of interfacial phenomena for materials in confined geometries, the high degree of polymerization N implies that the contribution of translational entropy of the molecules to the overall free energy[15,16] is weak relative to the effect of segment–segment and especially overall segment–surface interactions;[17] this can magnify the influence of surface-related effects.[17]

This is seen most directly in the basic Flory–Huggins model of polymer mixing, where the free energy of mixing ΔF_M (normalized per monomer volume) of two flexible polymers of degrees polymerization N_A and N_B is given by[15,16]

$$\Delta F_M/kT=(\phi_A/N_A)\ln\phi_A+(\phi_B/N_B)\ln\phi_B+\chi\phi_A\phi_B, \quad (1)$$

where ϕ_A and ϕ_B are the mean volume fractions of the two species and χ is a monomer–monomer interaction parameter. (In the usual assumption of incompressibility $\phi_A + \phi_B = 1$, and in what follows we write $\phi_A \equiv \phi$ and $\phi_B = 1 - \phi$.) The first two terms on the right-hand side of Eq. (1) are the translational entropy contributions; these are suppressed relative to their values in binary small molecule (or monomeric) mixtures by factors N_A and N_B, which are of the order 10^3–10^4 in high molecular weight polymers, while the intermolecular interaction contribution (in χ) remains comparable in both cases. The effects of both monomer–monomer interactions (in χ) and of monomer–surface interactions (see the later discussion) are thus magnified relative to the translational entropy effects in comparison with monomeric mixtures. The high degree of polymerization of the chain molecules has the further consequence of magnifying length scales of thermodynamically induced compositional variations, which is again convenient from an experimental viewpoint. For two polymer phases coexisting at temperatures T below T_c [for a binary mixture with an upper critical solution temperature (UCST)], the interfacial region separating them at equilibrium is characterized by a width w given by[18–20]

$$w=(\sqrt{2}a/3)(\chi-\chi_c)^{-1/2}, \quad (2)$$

where χ_c is the value of χ at $T = T_c$ and a is comparable with a monomer size. For polymers, χ_c is of order $(1/N)$ (N being the lesser of N_A and N_B) and this small value implies that there may be a wide range of χ values (and thus temperature) corresponding to $1 \gg \chi \gg \chi_c$, where the interfacial width w is of order of the polymer unperturbed dimensions $N^{1/2}a$. This can be hundreds of Ångstroms and enables measurements of w using direct spatial profiling methods.[14]

Isotopic polymer mixtures (such as of a polymer B with its deuterated analog A) provide a convenient model binary system. This is due in part to the low values of χ (which arise from the weak D/H differences[21,22]) which magnify spatial scales as discussed above, and also enables "fine tuning" of critical temperatures via choice of N; and partly it is due to the availability of experimental techniques which make use of deuterium labeling, such as infrared spectroscopy,[23] neutron,[24(a)] and ion-beam[24(b)] methods and nuclear reaction analysis,[25] which can be used to probe structural and dynamic properties of these mixtures. In addition, such an isotopic A/B mixture most closely conforms to the basic Flory–Huggins (FH) mean-field lattice model [as in Eq. (1)], which facilitates interpretation of the experimental observations. This is because the difference in monomeric structure (between A and B) is minimal, in line with the basic assumption of local structural symmetry inherent in the FH lattice model. In recent years, isotopic mixtures—primarily polystyrene $\{-[CH_2-CH(C_6H_5)-]_{N_B}$, hPS$\}$ and its deuterated analog $\{-[CD_2-CD(C_6D_5)-]_{N_A}$, dPS$\}$, but also other isotopic pairs have been widely studied. Small-angle neutron scattering (SANS) studies of compositional fluctuations in the dPS/hPS system in the one phase region ($T > T_c$) by Bates and co-workers[22] and Schwahn *et al.*[26] and measurement of thermodynamic slowdown of mutual diffusion in the same system by Green and Doyle[27] have been used to estimate the χ parameter for this mixture. More recently, Jones and co-workers have studied adsorption to an interface of dPS from a dPS/hPS mixture and were able to estimate monomer interaction parameters at the air interface.[28] All these studies were in the miscible region ($T > T_c$) of the phase diagram. Very recently, the coexistence characteristics in a dPS/hPS mixture were studied directly by Budkowski *et al.*[29] In these experiments, a relatively thick film of initially pure dPS was laid on an initially pure hPS film and the two species were allowed to interdiffuse to equilibrium at $T < T_c$ (i.e., in the two-phase region for this system which has a UCST). The resulting dPS concentrations $\phi_{1\infty}$ and $\phi_{2\infty}$ were determined in the two coexisting phases using nuclear reaction analysis (NRA) at several temperatures. The coexistence curve determined in these experiments is shown in Fig. 1. (It differs slightly from the curve predicted by the Flory–Huggins model with a ϕ-independent χ, as indicated; we return to this point later.)

The present study extends these earlier measurements on the dPS/hPS system (using the identical polymers for which the coexistence curve of Fig. 1 was determined) to the case where the thickness of the films is small; in particular, we investigate the effect of the finite thickness and the influence of surface effects on the coexisting composition profiles at $T < T_c$. In Sec. II, we describe the use of NRA to determine the composition profiles across the bilayer of coexisting dPS/hPS phases, in films of varying thickness, and for two different supporting surfaces. In Sec. III, we present the composition profiles in various configurations, and in Sec. IV, we analyze the behavior in terms of mean-field models using the experimentally extracted bulk and surface interaction parameters.

II. EXPERIMENT

Regular (or protonated) polystyrene (hPS) with weight averaged molecular weight $M_w = 2.89 \times 10^6$ and

Downloaded 24 Jun 2007 to 132.77.4.129. Redistribution subject to AIP license or copyright, see http://jcp.aip.org/jcp/copyright.jsp

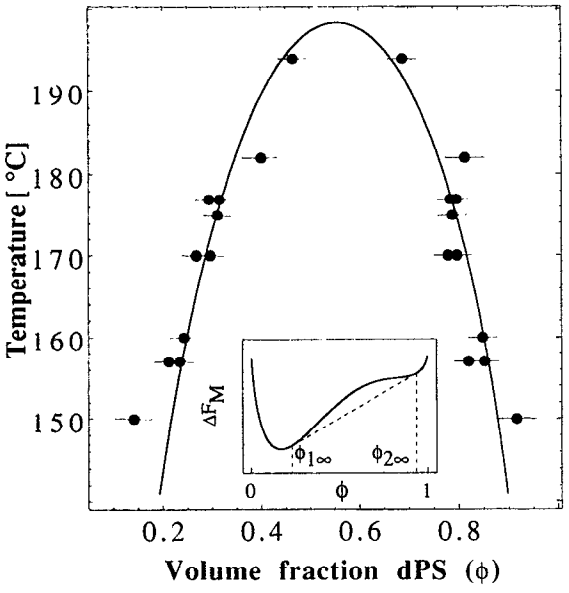

FIG. 1. The experimentally determined coexistence curve in the temperature-composition plane for the dPS/hPS couple used in the present experiments (from Ref. 29). The solid line is the coexistence curve calculated from the Flory–Huggins model [Eq. (1)] using a segment interaction parameter χ with a weak linear ϕ dependent as in Eq. (6). It represents the locus of contacts of the common tangent to the mixing free energy profile (see inset).

polydispersity $M_w/M_n = 1.09$ was obtained from Tosoh Corp. (Japan), and fully deuterated polystyrene (dPS) with $M_w = 1.03 \times 10^6$ and $M_w/M_n = 1.07$ was obtained from Polymer Laboratories (United Kingdom). Polished silicon wafers (obtained from Intel Electronics, Israel) were used as the supporting substrate, either following degreasing in toluene (Frutarom, analytical grade) (which leaves a thin SiO_2 layer on each wafer[30]), or following evaporation of a high-purity smooth gold layer (thickness >500 Å) onto the polished silicon wafers. Films (in the thickness range 200–600 nm) were spin cast from toluene solution either directly onto the substrate (either bare or gold-covered silicon), or were cast onto glass slides, floated on water, and picked up by the Si wafers bearing a precast film to form a bilayer. Both dPS/hPS/substrate and hPS/dPS/substrate geometries were used. In addition, a 23% dPS-composition blend was prepared and cast as a single film.

Wafers (size $\sim 1 \times 1.5$ cm^2) with the mounted films were sealed in glass ampoules under vacuum ($<10^{-5}$ Torr) and annealed in high-stability ovens for extended periods (up to one month) at 170 ± 0.5 °C. This is well below the critical temperature $T_c = 196 \pm 3$ °C for this system[29] (Fig. 1). Following the annealing period, the composition profiles of dPS normal to the substrate were determined using double NRA measurements as follows.

The use of NRA to monitor the composition profiles of deuterated species in polymer films has been described recently.[14,20,25,31] Briefly, a beam of charged ^{3}He ions is accelerated to an energy E_0 and is incident on the polymer film containing deuterated chains. The ions penetrate the film and undergo the reaction

$$^3\mathrm{He} + {}^2\mathrm{H} \rightarrow {}^4\mathrm{He} + {}^1\mathrm{H} + Q \quad (Q = 18.352 \text{ MeV}). \qquad (3)$$

The outgoing charged ^{4}He (α) particles are detected at a forward angle. The energy of these α particles depends on the depth within the sample at which the reaction takes place, as this determines both the energy of ^{3}He and the energy loss of the emerging ^{4}He before it reaches the detector. From the energy spectrum, and the calibrated reaction cross-section and energy loss within the samples, the relative composition-depth profile of the deuterium atoms (^{2}H) is determined. The method has a spatial resolution which is optimal [at ~ 14 nm fullwidth at half-maximum (FWHM)] at the sample surface for $E_0 = 700$ keV, but which even at a depth of several hundred nanometers is smaller than the coil dimensions of the polymer chains or than the typical spatial correlation or decay lengths in the conditions of our experiments. In order to determine absolute rather than relative compositions, the depth profiling is carried out in two stages (for each sample). First, an incident ^{3}He beam with $E_0 = 1.2$ MeV provides an unnormalized composition-depth profile with an effective depth range of ~ 1000 nm (at greater depths—with this value of E_0—the energy of the ^{3}He ions is so reduced by losses in penetrating the sample that the cross section for the nuclear reaction becomes prohibitingly low). Following this, a reference film (thickness 400 nm) of pure dPS is spin cast, floated, and mounted on top of the previously measured sample. NRA is then used again (with $E_0 = 1.6$ MeV and a corresponding depth limit ~ 1250 nm) to normalize the relative dPS composition in absolute units. An example is shown in Fig. 2. All profiles presented in Sec. III have been normalized in this fashion. We note also that once they have been measured, samples are not annealed and measured again. Each profile corresponds to a sample that has been annealed only once, measured (possibly at several points on its surface to yield several profiles), and then normalized as above.

III. RESULTS

Figure 3 shows a composition profile for relatively thick starting layers of dPS and hPS on silicon following 29.7 days of annealing at 170 ± 0.5 °C. (Very similar profiles were obtained in the context of the coexistence study carried out earlier.) The initial (unannealed) layers are indicated by broken lines and the two plateaus following annealing correspond (within the scatter) to the coexisting compositions $\phi_{1\infty}$ and $\phi_{2\infty}$ determined previously[29] and summarized in Fig. 1. At this temperature and for this geometry, the annealing time has been shown earlier[29] to be sufficiently long, so that the profiles are close to their equilibrium values. We note the small excess of dPS at the substrate interface. At this depth ($z \cong 900$ nm), the surface peak is smeared due to the relatively poor resolution [~ 50 nm half-width at half-maximum (HWHM)]. A more clear demonstration of dPS enrichment at the silicon surface is seen in Fig. 4, where a single film of initially uniform com-

Downloaded 24 Jun 2007 to 132.77.4.129. Redistribution subject to AIP license or copyright, see http://jcp.aip.org/jcp/copyright.jsp

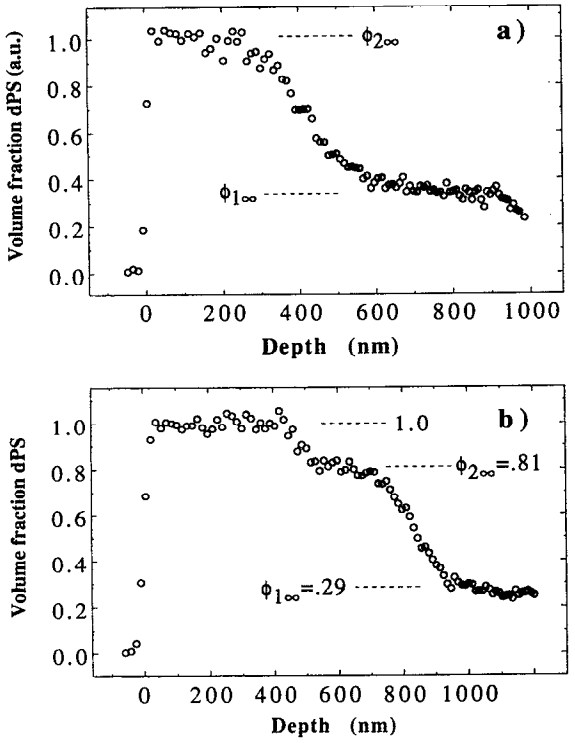

FIG. 2. (a) A composition-depth profile, determined by NRA (Ref. 25) for the dPS/hPS couple following interdiffusion of the originally pure (500 nm thick dPS and 510 nm thick hPS) layers at 170 °C for 18.8 days. The dPS volume fraction axis is unnormalized. (b) The same profile with a normalizing layer of pure dPS on top. The volume fraction of this layer establishes the $\phi_{\mathrm{dPS}}=1$ level and permits absolute values of the composition to be determined. All the profiles in this paper have been normalized in this way.

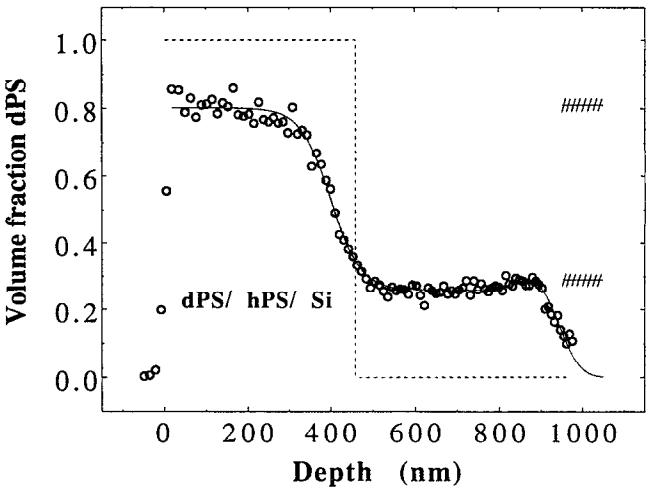

FIG. 3. Composition-depth profile of dPS (460 nm thick) hPS (500 nm thick) bilayer on Si substrate, annealed for 29.7 days at $T=170$ °C. The dashed step function indicates the initial unannealed profile, while the horizontal markers at 0.29 and 0.81 dPS volume fractions are the coexistence compositions $\phi_{1\infty}$ and $\phi_{2\infty}$ determined for this couple (Ref. 29) at 170 °C (see also Fig. 1). The solid line at the hPS–dPS interface corresponds to Eq. (5), while the solid line at the silicon interface (at $z\cong 950$ nm) is calculated as detailed in the text [and convoluted with the appropriate system resolution at this depth of 50 nm HWHM (Refs. 25 and 31)].

position 23% dPS has been annealed for 30 days at 170 °C. This composition is well within the one-phase regime at this temperature even though $T < T_c$ (Fig. 1). The profile shows a clear peak at the polymer–air interface (observed earlier for a different dPS/hPS system at $T > T_c$), but also a clear (if small) surface excess at the polymer–silicon interface.

Figure 5 shows the effect of limiting the thickness of the hPS layer (adjacent to the Si wall) to values comparable with the interfacial width w [Eq. (2)] between the coexisting phases on the one hand and the decay length of the surface enriched layer on the other. Following annealing for 27.7 days at $T=170$ °C (with the unannealed profiles shown as dashed lines), the initially pure hPS region "fills up," showing not only a clear surface peak due to dPS enrichment at the silicon interface, but also a "plateau" level—taken as the broad minimum around $z=680$ nm—whose composition (at ~34% dPS) appears significantly within the two-phase region (between the coexistence and spinodal lines) at this temperature (Fig. 1). Figure 6 indicates the time dependence of the dPS buildup. After some three days [Fig. 6(a)], the coexisting composition is reached, following in which the surface excess begins to be clearly observable [eight days, Fig. 6(b)], until the limiting (within our experimental parameters) profile Fig. 6(c) is observed, exceeding the coexistence level $\phi_{1\infty}$ at all points, and exhibiting a clear surface excess.

In contrast to this buildup of a surface excess on the bare silicon surface, Fig. 7 (following 17 days at 170 ±0.5 °C) and Fig. 8 (following 27.7 days at 170±0.5 °C) show that there is no tendency to a surface excess of dPS

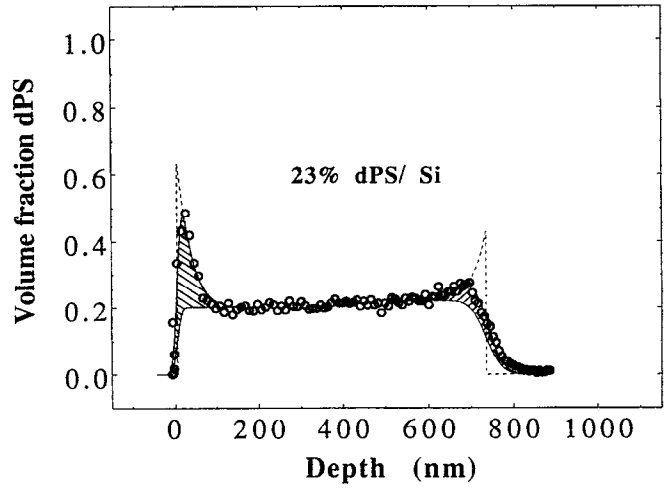

FIG. 4. Composition-depth profile of a thin film composed of 23% dPS/77% hPS on a Si substrate following 30 days annealing at $T=170$ °C. The broken lines are the calculated interface profiles (see the text for details) using $\mu_1=0.016$ Å and $g=-0.0076$ Å, with $\phi_\infty=0.20$ for the free interface ($z=0$) and $\mu_1=0.049$ Å, $g=-0.1$ Å, and $\phi_\infty=0.22$ for the silicon interface. The continuous lines represent the convolution of the calculated profiles with the appropriate resolution at the different depths. The shaded areas are the surface excess values Γ used in Fig. 11.

Downloaded 24 Jun 2007 to 132.77.4.129. Redistribution subject to AIP license or copyright, see http://jcp.aip.org/jcp/copyright.jsp

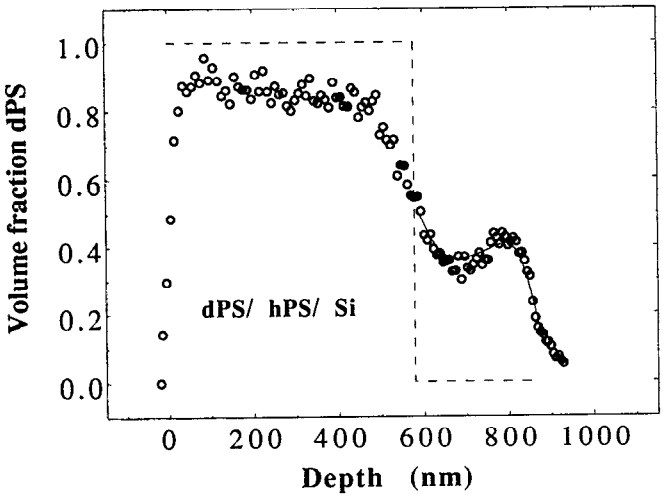

FIG. 5. The composition-depth profile of dPS (580 nm thick)–hPS (280 nm) bilayer on Si substrated following annealing for 27.7 days at $T = 170$ °C. The dashed line is the unannealed profiles. The solid curve at the Si interface is calculated (and convoluted with the appropriate system resolution) using μ_1 and g values as in Fig. 4, with $\phi_\infty = 0.34$.

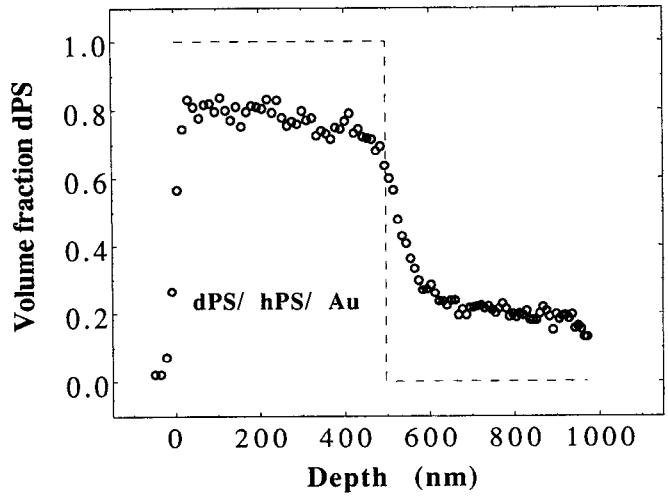

FIG. 7. The composition-depth profile for dPS (500 nm thick)–hPS (470 nm thick) bilayer on gold-coated Si wafers following 17 days annealing at $T = 170$ °C. Dashed lines are the unannealed bilayer.

when the Si substrate has been coated with gold. The initial configurations of the pure dPS and hPS films in Figs. 7 and 8 (broken lines) correspond very closely to these in Figs. 3 and 5, respectively (broken lines in those figures), but the annealed profiles are rather different for the bare as opposed to the gold-covered substrates. This is especially marked between Figs. 5 and 8 (as indicated by the solid line in Fig. 8). For the gold-coated substrate (Fig. 8), the plateau level in the dPS-poor phase—adjacent to the gold surface—does not exceed $\phi_{1\infty}$ at any point and (within our resolution) is quite flat at the polymer–solid interface, unlike the profile with the uncoated surface (Fig. 5 and the solid line in Fig. 8). There is a marked difference also at shorter times between the two types of substrate. The inset to Fig. 8 compares data for a bilayer annealed for seven days at 170±0.5 °C on a gold-covered substrate, with the corresponding profile (after eight days annealing at the same temperature and a similar bilayer configuration) for a bare Si surface. The surface peak on the latter substrate again contrasts with the absence of any dPS segregation on the gold.

Profiles of annealed bilayers with the reversed configuration (hPS/dPS/substrate) were also carried out; representative profiles are shown in Figs. 9 and 10 for different (thin) starting thicknesses of the pure hPS and dPS films, following 17 days annealing at 170±0.5 °C. We note two

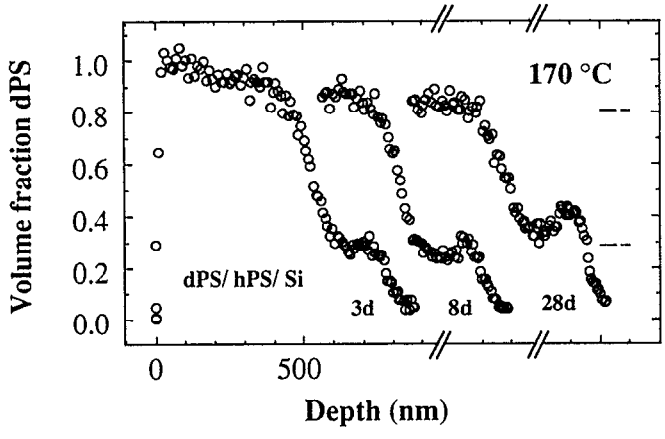

FIG. 6. Composition-depth profiles corresponding to the bilayer in Fig. 5 at progressive annealing times (a) 3; (b) 8; and (c) 28 days at 170 °C. Horizontal markers are the bulk coexistence levels (Ref. 29) $\phi_{1\infty}$ and $\phi_{2\infty}$ (see also Fig. 1).

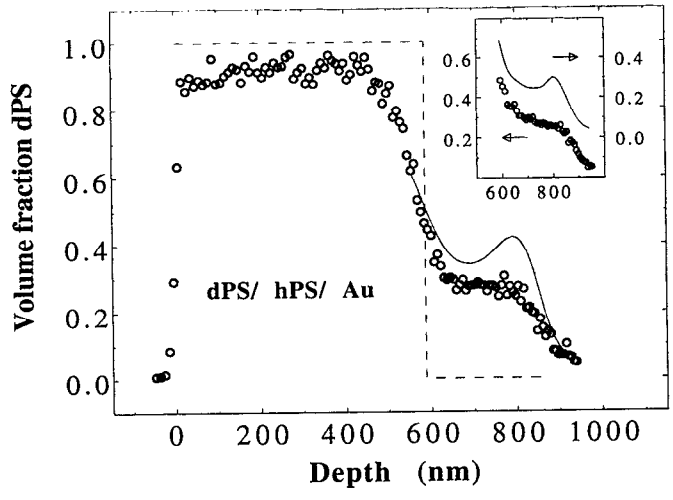

FIG. 8. Composition-depth profiles for dPS (500 nm thick)–hPS (270 nm thick) bilayer on gold-coated Si wafers following 27.7 days at $T = 170$ °C. The solid line near the substrate interface is taken from the corresponding profile on a bare Si substrate from Fig. 5. The dashed lines correspond to the unannealed bilayer. The inset shows a composition-depth profile from a different experiment following seven days annealing of the bilayer on a gold-coated Si wafer at $T = 170$ °C; the solid curve is for annealing on a bare Si substrate at the same temperature for eight days, taken from curve (b) of Fig. 6.

Downloaded 24 Jun 2007 to 132.77.4.129. Redistribution subject to AIP license or copyright, see http://jcp.aip.org/jcp/copyright.jsp

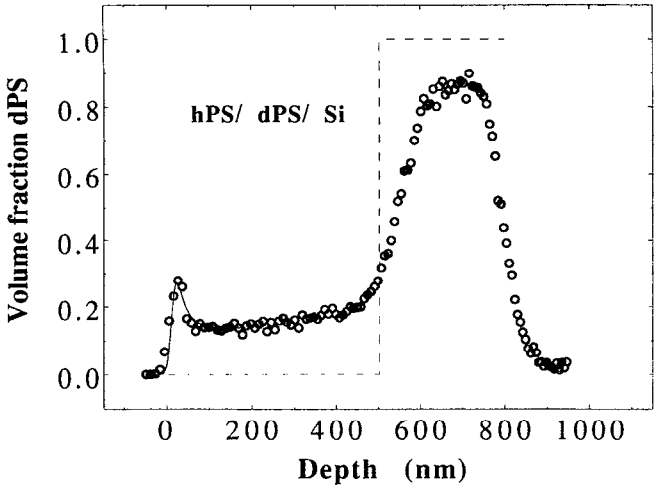

FIG. 9. The composition-depth profile of hPS (500 nm thick)–dPS (300 nm thick) bilayer on Si substrate following 17 days at $T=170$ °C. The dashed lines correspond to the unannealed layers. The solid line at the air interface is the calculated profile using μ_1 and g as in the caption to Fig. 4, with $\phi_\infty=0.137$ (suitably convoluted for instrumental resolution 10 nm HWHM at the surface).

qualitative features—the rate at which the plateau level of the dPS volume fraction increases in the initially pure hPS film depends both on the thickness of this film (as expected from simple diffusion considerations) and also on the ability of the initially pure dPS film (which acts as a dPS reservoir) to supply the deuterated chains. In Fig. 9, the initially pure dPS film is not able to "fill up" the hPS region to the coexistence concentration $\phi_{1\infty}$ without a shift of the original interface (vertical broken line) to the right as indicated. In Fig. 10, where the initially pure hPS film is thinner, a limitation arises because of the inadequate dPS reservoir in the initially thin pure dPS layer. In both cases,

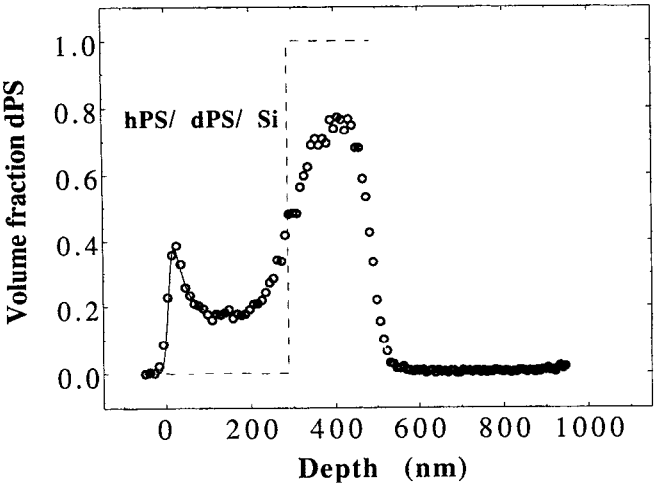

FIG. 10. The composition-depth profile for hPS (290 nm thick)–dPS (200 nm thick) bilayer on Si substrate following 17 days at $T=170$ °C. The solid line is the calculated (and convoluted as in Fig. 9) surface enrichment profile using the bare surface interaction parameter as in Fig. 4 and with $\phi_\infty=0.175$. Dashed lines are unannealed bilayers.

the effect is to prevent the plateau level in the dPS-poor phase (adjacent to the polymer–air interface peak at $z=0$) from reaching $\phi_{1\infty}$ in the annealing time. Nonetheless, well-developed surface peaks at the polymer–air interface are observed in both cases, which appear to be in equilibrium with the adjacent plateau levels of dPS in the dPS-poor phase. We return to this point in the following section.

IV. DISCUSSION

A good starting point for a quantitative interpretation of the profiles of coexisting phases in thin films, together with surface interaction effects, is the generalized method due to Cahn and Hilliard[32] (though a similar approach was used already by van der Waals[33] much earlier, and in a slightly different context also by Landau and Ginsburg[34]) for analyzing interfacial profiles at phase boundaries. The method was originally developed in the context of metallic or small-molecule binary mixtures and essentially involves minimizing the overall free energy with respect to the composition profile across the interfaces. The Cahn–Hilliard approach has been extended to polymeric systems by several workers;[35–40] here we largely follow the notation of Schmidt and Binder.[40] In the long-wavelength limit[41] (and ignoring possible effects due to long-ranged dispersion forces[9]), the free energy excess in the bulk for two semi-infinite polymer phases A and B separated by a planar interface (at $z=0$) per unit area of the interface is given by $\Delta F_{b,i}$, where

$$\Delta F_{b,i}/kT=\int_{-\infty}^{\infty} dz\left[\Delta F_M-\Delta\mu\phi+\frac{a^2}{36\phi(1-\phi)}(\nabla\phi)^2\right], \tag{4}$$

where ΔF_M is the mixing free energy given by Eq. (1), $\Delta\mu$ is the chemical potential difference, $\phi\{\equiv\phi(z)\}$ is the local volume fraction of component A and the gradient term is with respect to z [we note that for polymers, in contrast to small molecule systems, the squared gradient term in Eq. (4) is due mainly to entropic rather than enthalpic effects[42]]}. For coexistence in the two-phase region ($\chi > \chi_c$, or $T < T_c$ for an UCST), the coexisting compositions are $\phi_{1\infty}$ and $\phi_{2\infty}$. The values of $\phi_{1\infty}$ and $\phi_{2\infty}$ are obtained by minimizing the right-hand side of Eq. (4) far from the interface, in a region where $\nabla\phi\to 0$. Minimization of $\Delta F_{b,i}$ with respect to the composition profile $\phi(z)$, subject to the boundary conditions of the phase compositions $\phi_{1\infty}$, $\phi_{2\infty}$ at $z=\pm\infty$, yields the standard result for the profile

$$\phi(z)=1/2[(\phi_{1\infty}+\phi_{2\infty})+(\phi_{1\infty}-\phi_{2\infty})\tanh(z/w)] \tag{5}$$

with the characteristic width w given by Eq. (2). While Eqs. (2) and (5) are derived analytically only for the symmetric case $N_A=N_B$ (for which $\phi_{1\infty}=1-\phi_{2\infty}$), they can be shown[43] to be very good approximate forms also for $N_A\neq N_B$, as long as the ratio (N_A/N_B) is not too different from unity, as is true in the present experiments (where $N_A/N_B\cong 0.3$). Such a profile is calculated for the interface between the coexisting plateaus of dPS-rich and hPS-rich

Downloaded 24 Jun 2007 to 132.77.4.129. Redistribution subject to AIP license or copyright, see http://jcp.aip.org/jcp/copyright.jsp

phases in Fig. 3. No adjustable parameters are used; both the coexisting compositions and the value of χ for this pair are taken from the direct study of coexistence described earlier.[29] In this system, the value of χ which describes the experimentally determined coexistence curve reproduced in Fig. 1 has a weak linear ϕ dependence[44]

$$\chi(\phi,T)=[(0.124/T)-1.06\times10^{-4}](1-0.18\phi). \quad (6)$$

The calculated profile is convoluted with the system resolution at this depth to yield the solid line shown in Fig. 3 between the coexisting plateaus.

For the case of a polymer mixture in contact with a solid wall at $z=0$, similar considerations apply, except that the overall free energy now consists both of a bulk contribution ΔF_b (per unit area normal to the surface) and a specific "bare" surface contribution ΔF_s (per unit area). ΔF_b is now summed over the half-space ($z>0$) from the wall

$$\Delta F_b/kT=\int_0^\infty dz\left[\Delta F_M-\Delta\mu\phi+\frac{a^2}{36\phi(1-\phi)}(\nabla\phi)^2\right]. \quad (7)$$

The bare surface contribution (to distinguish it from the bulk contribution at $z=0$) is frequently approximated[45] by the first two terms of an expansion in the volume fraction at the surface ϕ_s [$\equiv\phi(z=0)$]

$$-\Delta F_s/kT=\mu_1\phi_s+\tfrac{1}{2}g\phi_s^2. \quad (8)$$

Physically, μ_1 is regarded as the chemical potential difference favoring the presence of species A (volume fraction ϕ) at the surface, while g represents the effect of change in surface interactions (including different coordination numbers between A monomers at the surface). The composition profile $\phi(z)$ from the surface to the bulk composition ϕ_∞ (say) of the one-phase mixture adjacent to it is obtained via the minimization with respect to $\phi(z)$ and ϕ_s of

$$\frac{\Delta F_b+\Delta F_s}{kT}=\int_0^\infty\left[\Delta F_M-\Delta\mu\phi+\frac{a^2}{36\phi(1-\phi)}(\nabla\phi)^2\right]dz-\mu_1\phi_s-\frac{1}{2}g\phi_s^2. \quad (9)$$

For a film composed of a mixture in the one-phase regime on a solid substrate, as shown in Fig. 4 for ϕ ($\equiv\phi_A$, volume fraction of dPS) $=23\%$, the effects of the surface interactions result in dPS enrichment both at the polymer–air and at the polymer–silicon interfaces. Clearly, different pairs of parameters μ_1 and g may apply for each type of interface. For the situation shown in Fig. 5, where coexistence between the dPS-rich and hPS-rich phases is perturbed significantly by the surface excess, the process may be described qualitatively as follows: the initially pure dPS layer (adjacent to the air interface) interdiffuses into the initially pure hPS layer, tending to create an interface of finite width w between two coexisting phases, as is the case in Fig. 3. However, the closer proximity of the solid (silicon) surface, with its preferential attraction for the dPS chains, perturbs the profile given by Eq. (5). In principle, the full profile shown in Fig. 5 should be calculable by a suitable minimization of the total excess free energy of the system subject to the boundary conditions at the air and solid surfaces; these depend on the bulk interaction parameter χ and the bare surface interaction parameters μ_1 and g (but these parameters can be obtained independently as shown below). We do not at present know how to do this in an *a priori* fashion and adopt instead a slightly different approach for a more quantitative analysis of our data. This is based on the assumption that the composition profiles $\phi(z)$ in the vicinity of an interface (either polymer–air or polymer–substrate) are in equilibrium with respect to the plateau value of ϕ in the region adjacent to the respective interface-enriched profile. There is some theoretical justification for this from the recent work of Binder and Frisch[46] on the dynamics of surface enrichment from a binary mixture; their work indicates local equilibrium of this sort as long as the spatial extent of the plateau in composition adjacent to the surface peak is comparable with or greater than the coil dimensions of the polymer (within the slow-fluctuation limit of the present treatment). This condition is generally met in the confined coexistence profiles in the present discussion; a similar assumption has been used by Jones and Kramer[47] in their analysis of the kinetics of surface aggregation from a dPS/hPS mixture.

With this in mind, we proceed as follows: the total excess free energy of the system with an adsorbing interface at $z=0$ (taken locally at either the air or substrate) finds its minimum for the concentration profile $\phi(z)$ given implicitly by[40]

$$z=\frac{a}{6}\int_{\phi=\phi_s}^{\phi=\phi(z)}\{\phi(1-\phi)[\Delta F_M(\phi)-\Delta F_M(\phi_\infty)-\Delta\mu(\phi-\phi_\infty)]\}^{-1/2}d\phi. \quad (10)$$

Here ΔF_M is the Flory–Huggins mixing free energy of Eq. (1); ϕ_s is the (dPS) volume fraction at the interface whose value is determined by μ_1 and g; ϕ_∞ is the plateau value of the bulk concentration as discussed above, while $\Delta\mu$ is the exchange chemical potential $\partial\Delta F(\phi_\infty)/\partial\phi$. The expression in Eq. (10) describes implicitly the variation of the composition profile $\phi(z)$ from ϕ_∞ to its value ϕ_s at the surface. ϕ_s may be determined by the Cahn construction[48] expressed by the condition

$$-\frac{\partial(\Delta F_s/kT)}{\partial\phi_s}=\mu_1+g\phi_s=\frac{a}{3}\{[\Delta F_M(\phi_s)-\Delta F_M(\phi_\infty)-\Delta\mu(\phi_s-\phi_\infty)]/\phi_s(1-\phi_s)\}^{1/2}. \quad (11)$$

The shape of $\phi(z)$ is determined then via Eq. (10) by the bulk plateau value ϕ_∞, the cutoff value ϕ_s at the surface, and by the interaction parameter χ via ΔF_M. $\chi(\phi,T)$ for this particular isotopic pair is known from our earlier study[29] [Fig. 1 and Eq. (6)] and ϕ_∞ is obtained directly from the plateau compositions of the profiles, while μ_1 and g—which determine ϕ_s—may be obtained as follows from the surface excess Γ of the dPS at each interface defined as

Downloaded 24 Jun 2007 to 132.77.4.129. Redistribution subject to AIP license or copyright, see http://jcp.aip.org/jcp/copyright.jsp

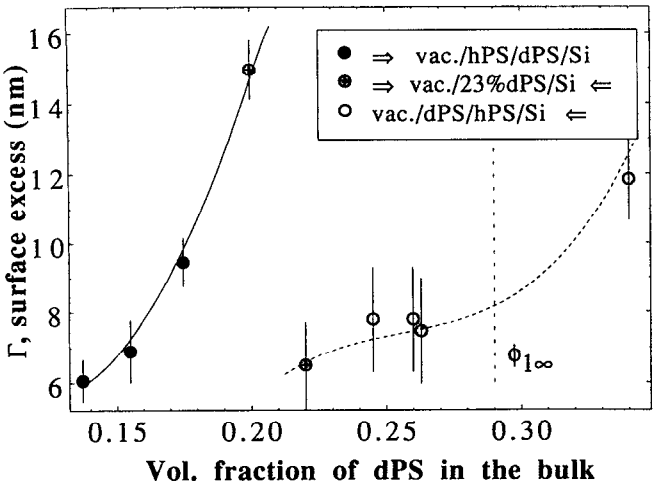

FIG. 11. A variation of dPS excess Γ at the vacuum (solid circles) and silicon (empty circles) interfaces as a function of ϕ_∞ determined for several profiles (Figs. 3–5, 9, and 10 and others not shown) as indicated by shaded areas in Fig. 4 (the data from Fig. 4 is given by the crossed circles). The vertical broken line at 0.29 dPS volume fraction corresponds to $\phi_{1\infty}$. The respective continuous curves are the calculated variations (see the text) using the appropriate bare surface interaction parameters for the two types of interface, as given in the text and in the caption to Fig. 4.

$$\Gamma = \int_0^{z(\phi_\infty)} [\phi(z) - \phi_\infty] dz. \tag{12}$$

Here $z(\phi_\infty)$ is the distance from the surface to the plateau in composition. We use a procedure described earlier.[28,40] The surface excess Γ is determined at each appropriate value of the plateau composition ϕ_∞ adjacent to the interface-enriched region. This is done (as indicated by the shaded regions in Fig. 4) for both polymer–air and polymer–substrate interfaces for all profiles, and the results are shown in Fig. 11. For each of these values of ϕ_∞ Γ is plotted against ϕ_s [$=\phi(z=0)$] from Eq. (12), and the actual surface excess at the appropriate ϕ_∞ value is used to read off the corresponding surface concentration ϕ_s. Finally, using the Cahn construction, the quantity $-(\partial \Delta F_s/\partial \phi_s)$ from the right-hand side of Eq. (11) is plotted for each value $\phi_s(\phi_\infty)$ defining the line $(\mu_1 + g\phi_s)$. This is shown in Fig. 12 for both types of interfaces in the present study. From these data, the best-fit lines yield values of the "bare-surface" parameters $\mu_1 = (0.016 \pm 0.002)$ Å and $g = -(0.0076 \pm 0.0020)$ Å for the free dPS/hPS surface (this compares with earlier[28] mean values $\mu_1 = 0.024$ Å and $g = -0.0046$ Å, extracted for the dPS/hPS system); and $\mu_1 = (0.049 \pm 0.008)$ Å and $g = -(0.1 \pm 0.02)$ Å for the interface between the silicon surface and the polymer mixture. We now have all the parameters necessary for solution of Eqs. (10) and (12), and these are solved to yield both the explicit composition profiles $\phi(z)$ at the two interfaces and the Γ (ϕ_∞) dependence. These calculated values are presented in Figs. 3–5, 9, and 10 for the profiles (following the convolution of calculated profiles with the appropriate instrumental resolution at the respective depths), and in Fig. 11 for $\Gamma(\phi_\infty)$. We note a

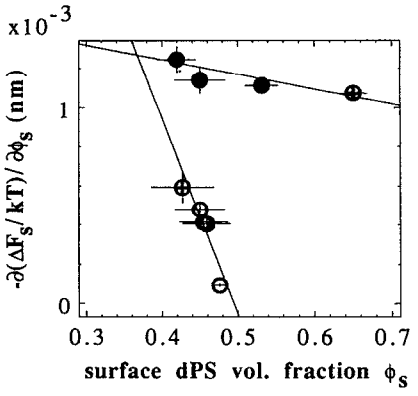

FIG. 12. The Cahn construction (Ref. 48) for surface enrichment at the hPS–dPS/vacuum and hPS–dPS/silicon interfaces for our system as described in the text. The two sets of points correspond to those in Fig. 11. The straight lines are the regression lines going through the data corresponding to $(\mu_1 + g\phi_s)$ for the two sets of bare surface parameters μ_1 and g.

satisfactory agreement of calculated with measured profiles and surface excess, indicating the self-consistency of our procedure.

Before summarizing, we remark on a number of points. The values of the bare-surface virial coefficients μ_1 and g for the polymer/air interface are reasonably close to those derived by Jones *et al.* for a dPS/hPS mixture. The small differences may be due to (a) the different temperatures used. In particular, we worked at $T < T_c$, while their experiments were at $T > T_c$. (b) We used a χ parameter which has a slight ϕ dependence determined from the directly measured coexistence curve for our particular system (Fig. 1) (the values of μ_1 and g depend on the χ used), while they used a ϕ-independent χ parameter derived from small-angle neutral scattering (SANS).[22]

The values of μ_1 and g for the polymer–silicon surface deserve comment. Here the value of g is much larger than at the air interface, which is a little surprising since g is conceptually related to the "missing neighbors" effect.[40] One possible reason for this may have to do with the different nature of the interfaces themselves: the air interface is soft—at $T > T_g$—and may accommodate local reorganization of the PS monomers in a way which the rigid silicon interface does not, thereby reducing the missing neighbors effect. We also remark on the unexpected relative magnitudes $|g| > |\mu_1|$. This may well have to do with the fact that while μ_1 and g are used for the low ϕ_s limit of ΔF_s, the values deduced (from Fig. 12) are in fact an extrapolation from a limited range of relatively high values of ϕ_s.

Finally, we note the qualitative feature of a marked excess dPS adsorption at the silicon interface. This contrasts with the dPS depletion at a silicon interface suggested by recent neutron reflectrometry studies.[49] This difference may be due to the different treatment of the silicon wafers, which in our studies were merely cleaned (leaving a thin SiO_2 layer on the surface), while in the study suggesting a possible dPS depletion, the Si wafers were etched,

Downloaded 24 Jun 2007 to 132.77.4.129. Redistribution subject to AIP license or copyright, see http://jcp.aip.org/jcp/copyright.jsp

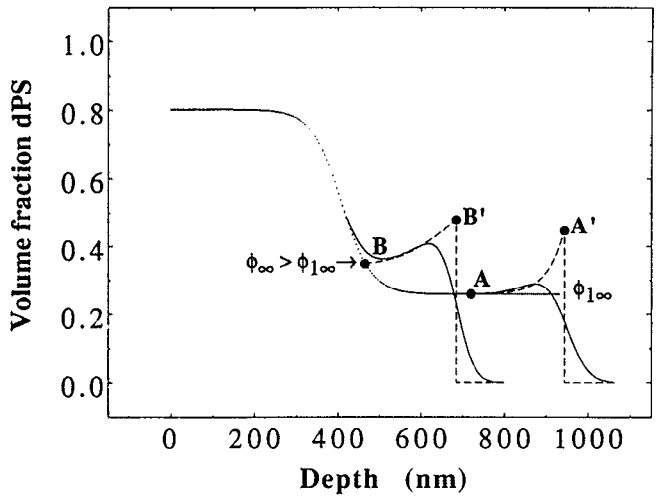

FIG. 13. Summarizing the effect on the coexistence profile of confining our binary isotopic mixture to thin films. The dotted line about $z=400$ nm is the bulk interface profile corresponding to Eq. (5) and calculated also for Fig. 3. The enrichment profile A–A' is for bilayers sufficiently thick that $\phi_\infty = \phi_{1\infty}$ and corresponds to the actual data in Fig. 3. For thin films, the surface enrichment at the Si substrate follows the curve B–B', where the "plateau" in composition at ϕ_∞ exceeds the bulk coexistence value $\phi_{1\infty}$. This curve corresponds exactly to Fig. 5. Solid lines are the convolutions of the calculated (broken) profiles with the system resolution at the appropriate depths. All curves are calculated with the parameter derived for our particular dPS/hPS couple.

probably removing the oxide layer. The reason for this may have to do with the different extent to which dPS and hPS interact with oxide species on the silicon surface in the unetched case, as suggested by the marked isotope effects in studies of phase separation in hPS/poly(vinyl methyl ether) blends compared with dPS/poly(vinyl methyl ether) blends.[50]

To conclude, our study shows that the composition profile across two coexisting, thin polymer films may be modified by the finite thickness of the films as well as specific interactions with the confining interfaces. The results are interpreted in terms of a Flory–Huggins mixing energy model (which is probably rather good for the isotropic binary mixture studied), using an interaction parameter determined from a direct coexistence study of this system, together with an approximate bare-surface interaction term. The results may be summarized as shown schematically in Fig. 13. For thick layers, two essentially independent regions may be identified—an interface between the coexisting phases spanning the coexisting compositions $\phi_{1\infty}$ and $\phi_{2\infty}$ together with a surface-enriched region spanning the compositions $\phi_{1\infty}$ and ϕ_s at the substrate surface (dotted line in Fig. 13). For the case where the dimension of the phase adjacent to the adsorbing surface becomes sufficiently thin, the two distinct regions become coupled and the composition of lowest energy (assuming our data correspond to the equilibrium situation) is now one where the coexisting plateau composition at composition ϕ_∞ (point B in Fig. 13) is driven into the miscibility gap of the bulk phase diagram, i.e., $\phi_\infty > \phi_{1\infty}$. This effect is observed only where the confining substrate interface tends to adsorb one of the species preferentially (in the present investigation, it occurs for bare silicon, but not when it is coated with gold); it may be related to the different coexistence behavior observed on different substrates[12,13] when thin films of binary polymeric mixtures are taken from the one-phase to the two-phase region.

ACKNOWLEDGMENTS

We thank the German–Israel Foundation (G.I.F.) and the U.S.–Israel Binational Science Foundation for support of this work and K. Binder and P. Pincus for very helpful discussions.

[1] For some recent reviews, see *Physics and Chemistry in Restricted Geometries*, edited by J. Klafter and J. Drake, Isr. J. Chem. **31**, No. 2 (1991).
[2] See *Liquids at Interfaces* (*Les Houches Session XLVIII*), edited by J. Charvolin, J-F. Joanny, and J. Zinn-Justin (North–Holland, Amsterdam, 1990).
[3] *Molecular Dynamics in Restricted Geometries*, edited by J. Klafter and S. Drake (Wiley, New York, 1989), and references therein.
[4] M. E. Fisher and P. G. de Gennes, C.R. Acad. Sci. Ser. B **287**, 207 (1978).
[5] M. E. Fisher and H. Nakanishi, J. Chem. Phys. **75**, 5857 (1981); H. Nakanishi and M. E. Fisher, *ibid.* **78**, 3279 (1983).
[6] S. Mader, Thin Solid Films, **35**, 195 (1976).
[7] K. Kremer, J. Phys. **47**, 1269 (1986).
[8] T. L. Hill, *Thermodynamics of Small Systems* (Benjamin, New York, 1963); Vol. 1, p. 82.
[9] See, e.g., P. G. de Gennes, Rev. Mod. Phys. **57**, 827 (1985), and references therein; also S. Dietrich and M. Schick, Phys. Rev. B **31**, 478 (1985).
[10] B. A. Scheibner, M. R. Meadows, R. C. Mockler, and W. J. O'Sullivan, Phys. Rev. Lett. **43**, 590 (1979).
[11] M. R. Meadows, B. A. Scheibner, R. C. Mockler, and W. J. O'Sullivan, Phys. Rev. Lett. **43**, 492 (1979).
[12] Y. Cohen, M.Sc. thesis, Weizmann Institute, 1980.
[13] S. Reich and Y. Cohen, J. Polym. Sci.: Polym. Phys. **19**, 1255 (1981).
[14] J. Klein, Science **250**, 640 (1990).
[15] P. J. Flory, *Principles of Polymer Chemistry* (Cornell University, Ithaca, N.Y., 1975).
[16] P. G. de Gennes, *Scaling Concepts in Polymer Physics* (Cornell University, Ithaca, N.Y., 1979).
[17] See, e.g., J. Klein, in *Liquids at Interfaces, 1988 Les Houches Summer School Series XLVIII,* edited by J. Charvolin, J-F. Joanny, and J. Zinn-Justin (North–Holland, Amsterdam, 1990); p. 232.
[18] E. Helfand and Y. Tagami, J. Chem. Phys. **56**, 3592 (1971).
[19] L. Leibler, Macromolecules **15**, 1283 (1982); K. Binder, J. Chem. Phys. **79**, 6387 (1983).
[20] U. K. Chaturvedi, U. Steiner, O. Zak, G. Krausch, and J. Klein, Phys. Rev. Lett. **63**, 616 (1989).
[21] A. D. Buckingham and H. G. Hentschel, J. Polym. Sci.: Polym. Phys. **18**, 853 (1980).
[22] F. S. Bates and G. D. Wignall, Phys. Rev. Lett. **57**, 1429 (1986).
[23] J. Klein, Nature **274**, 143 (1978).
[24] (a) See, e.g., T. Russell, Mater. Sci. Rep. **5**, 171 (1990), and references therein; (b) E. J. Kramer, Phys. Status Solidi B **173**, 189 (1991).
[25] U. K. Chaturvedi, U. Steiner, O. Zak, G. Krausch, G. Schatz, and J. Klein, Appl. Phys. Lett. **56**, 1228, (1990).
[26] D. Schwahn, K. Hahn, J. Streib, and T. Springer, J. Chem. Phys. **93**, 8393 (1990).
[27] P. F. Green and B. L. Doyle, Phys. Rev. Lett. **57**, 2407 (1986).
[28] R. A. L. Jones, E. J. Kramer, M. H. Rafailovich, J. Sokolov, and S. Schwarz, Phys. Rev. Lett. **62**, 280 (1989).
[29] A. Budkowski, U. Steiner, G. Schatz, and J. Klein, Europhys. Lett. **18**, 705 (1992).
[30] S. M. Sze, *Semiconductor Devices* (Wiley, New York, 1985), Chap. 9.
[31] U. Steiner, G. Krausch, G. Schatz, and J. Klein, Phys. Rev. Lett. **64**, 1119 (1990); U. Steiner, U. K. Chaturvedi, O. Zak, G. Krausch, G.

Downloaded 24 Jun 2007 to 132.77.4.129. Redistribution subject to AIP license or copyright, see http://jcp.aip.org/jcp/copyright.jsp

Schatz, and J. Klein, Makromol. Chem., Macromol. Symp. **45**, 283 (1991).
[32] J. Cahn and J. Hilliard, J. Chem. Phys. **28**, 258 (1958).
[33] J. D. van der Waals, Verh. K. Akad. Wet. Sect. I. **1** (1893).
[34] See L. D. Landau and E. J. Lifshitz, *Statistical Physics*, 3rd ed. (Pergamon, Oxford, 1980).
[35] A. Vrij, J. Polym. Sci. A-2 **6**, 1919 (1968).
[36] E. Helfand and A. M. Sapse, J. Chem. Phys. **62**, 1327 (1975).
[37] P. G. de Gennes, Macromolecules **14**, 1137 (1981).
[38] H. Nakanishi and P. Pincus, J. Chem. Phys. **79**, 997 (1983).
[39] J. Klein and P. Pincus, Macromolecules **15**, 1129 (1982).
[40] I. Schmidt and K. Binder, J. Phys. **46**, 1631 (1985).
[41] For polymers, this condition corresponds to $\nabla\phi < (Na^2)^{-1/2}$.
[42] P. G. de Gennes, J. Chem. Phys. **72**, 4756 (1981).
[43] A. Budkowski, U. Steiner, G. Schatz, and J. Klein (to be published).
[44] A linear dependence is used as the simplest nontrivial modification to the case of a ϕ-independent χ parameter.
[45] This is equivalent to assuming both a low ϕ_s and an absence of long-ranged surface interactions (Ref. 9).
[46] K. Binder and H. L. Frisch, Z. Phys. B: Condensed Matter **84**, 403 (1991); K. Binder (private communication); see also R. Lipowski and D. A. Huse, Phys. Rev. Lett. **52**, 353 (1986).
[47] R. A. L. Jones and E. J. Kramer, Philos. Mag. B **62**, 129 (1990).
[48] J. W. Cahn, J. Chem. Phys. **66**, 3667 (1977).
[49] R. A. L. Jones, E. J. Kramer, L. J. Norton, K. Shull, G. P. Felcher, A. Karim, and L. J. Fetters (to be published).
[50] F. Ben Cheik Larbi, S. Leloup, J. L. Halary, and L. Monnerie, Polym. Commun. **27**, 23 (1986).

Downloaded 24 Jun 2007 to 132.77.4.129. Redistribution subject to AIP license or copyright, see http://jcp.aip.org/jcp/copyright.jsp